LEGIBILITY NOTICE

A major purpose of the Technical Information Center is to provide the broadest dissemination possible of information contained in DOE's Research and Development Reports to business, industry, the academic community, and federal, state and local governments.

Although a small portion of this report is not reproducible, it is being made available to expedite the availability of information on the research discussed herein.

LA-UR -85-2195

1985

CONF-8506128-2

Los Alamos National Laboratory is operated by the University of California for the United States Department of Energy under contract W-7405-ENG-36

LA-UR--85-2195

DE85 014087

TITLE MIXED-MODE FRACTURE OF CERAMICS

AUTHOR(S) J. J. Petrovic

SUBMITTED TO FOURTH INTERNATIONAL SYMPOSIUM on the FRACTURE MECHANICS OF CERAMICS, Virginia Polytechnic Institute and State University, Blackburg, VA
June 19-21, 1985

DISCLAIMER

Los Alamos Los Alamos National Laboratory
Los Alamos, New Mexico 87545

MIXED-MODE FRACTURE OF CERAMICS

J. J. Petrovic

Materials Science and Technology Division
Los Alamos National Laboratory
Los Alamos, New Mexico 87545

ABSTRACT

The mixed-mode fracture behavior of ceramic materials is of importance for monolithic ceramics in order to predict the onset of fracture under generalized loading conditions and for ceramic composites to describe crack deflection toughening mechanisms. Experimental data on surface flaw mixed-mode fracture in various ceramics indicate that the flaw-plane normal stress at fracture decreases with increasing in-flaw-plane shear stress, although present data exhibit a fairly wide range in details of this $\sigma - \tau$ relationship. Fracture from large cracks suggests that Mode II has a greater effect on Mode I fracture than Mode III. A comparison of surface flaw and large crack mixed-mode I-II fracture responses indicates that surface flaw behavior is influenced by shear resistance effects.

INTRODUCTION

The mixed-mode fracture behavior of fracture-initiating flaws in ceramic materials is of importance for two reasons. First, this is the necessary basis of realistic, physically-based multiaxial loading fracture criteria for monolithic ceramics with a statistical flaw distribution (1,2). Secondly, such behavior is intimately related to crack deflection toughening mechanisms in ceramic composites (3). The purpose of the present paper is to review experimental mixed-mode fracture results for ceramics and other brittle materials, and to compare these results to the predictions of present theoretical mixed-mode fracture criteria in order to determine their applicability.

MIXED-MODE FRACTURE THEORIES

The three Modes of fracture are shown in Figure 1. Mode I, the opening mode, exhibits crack surface displacements perpendicular to the crack plane. Mode II, the sliding mode, exhibits crack surface displacements in the plane of the crack and perpendicular to the crack front. Mode III, the tearing mode, exhibits crack surface displacements also in the plane of the crack but parallel to the crack front. Generalized loading conditions will involve combined Modes I, II, and III. The different fracture Modes produce different stress distributions in the

material ahead of the crack tip, the intensity of which are governed by the stress intensity factors K_I, K_{II}, and K_{III}.

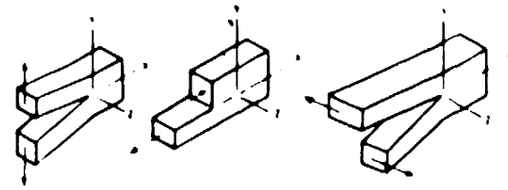

MODE I MODE II MODE III

Mode I: $\begin{matrix}\sigma_{xx}\\ \sigma_{yy}\\ \sigma_{xy}\end{matrix} = \frac{K_I}{(2\pi R)^{1/2}} f(\theta)$

Mode II: $\begin{matrix}\sigma_{xx}\\ \sigma_{yy}\\ \sigma_{xy}\end{matrix} = \frac{K_{II}}{(2\pi R)^{1/2}} f(\theta)$

Mode III: $\begin{matrix}\sigma_{xz}\\ \sigma_{yz}\end{matrix} = \frac{K_{III}}{(2\pi R)^{1/2}} f(\theta)$

$K_I \propto (\sigma_{yy})_R \cdot C^{1/2}$

$K_{II} \propto (\sigma_{xy})_R \cdot C^{1/2}$

$K_{III} \propto (\sigma_{zy})_R \cdot C^{1/2}$

C = Crack length

$(\sigma_{ij})_R$ are remote stresses

FIGURE 1: The Three Modes of Fracture.

The simplest mixed-mode fracture criterion is the coplanar criterion (4). This criterion assumes that mixed-mode fracture will initiate, with crack extension in the plane of the initial crack, when the strain energy release rate in this plane reaches a critical value (this critical value is taken to be a material parameter equal to the pure Mode I critical strain energy release rate). However, coplanar mixed-mode fracture is virtually never observed and so non-coplanar strain energy release rate criteria have been put forward (5-10). In non-coplanar strain energy release rate criteria, the mixed-mode crack is presumed to extend in the non-coplanar direction of maximum strain energy release rate, when this quantity reaches a critical value. Two other criteria of non-coplanar mixed-mode fracture are the maximum tangential tensile stress theory (11) and the strain energy density theory (12). The maximum tangential tensile stress theory assumes that crack extension starts in the plane perpendicular to the direction of greatest crack tip tangential tension σ_θ, with catastrophic fracture occurring when the quantity $(2R)^{\frac{1}{2}}\ \sigma_\theta$ reaches a critical value. It is interesting to note that the strain energy release rate theory of Nuismer (6) yields the same predictions as the maximum tangential tensile stress theory. The strain energy density theory assumes that crack initiation will start in a radial direction along which the strain energy density is minimum, with fracture occurring when the strain energy density factor reaches a critical value.

The predictions of a number of these criteria for mixed-mode I-II fracture are shown in Figure 2. These theories predict that K_I decreases

with increasing K_{II}. It should be noted that these criteria also predict values of the ratio K_{IIC}/K_{IC} for the case of pure Mode II fracture. For the various mixed-mode fracture theories, the range of predictions is $0.63 \leq K_{IIC}/K_{IC} \leq 1.02$.

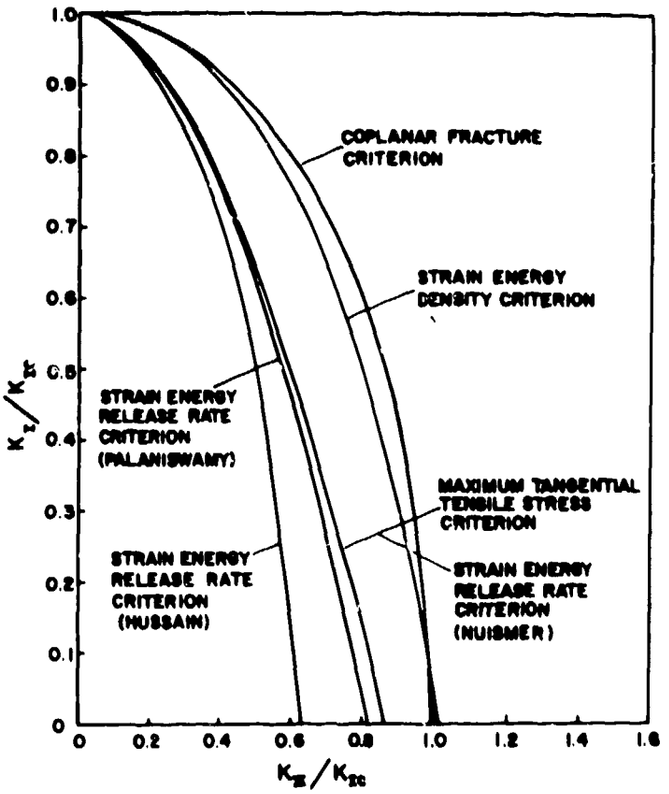

FIGURE 2: Predictions of Theoretical Mixed-Mode Fracture Criteria.

EXPERIMENTAL MIXED-MODE FRACTURE RESULTS

Indentation Surface Flaws

The mixed-mode fracture of ceramics has been examined largely using indentation surface flaws under various loading configurations. Experimental results of all studies to date are summarized in Figure 3. A key for the experimental data is given in Table 1. In Figure 3, σ_n/σ_o is plotted versus τ/σ_o, where σ_n is the stress normal to the flaw plane, τ is the shear stress in the plane of the flaw, and σ_o is the fracture stress under pure Mode I conditions.

Except for one data point, the data in Figure 3 indicate that σ_n/σ_o at fracture decreases with increasing τ/σ_o. This means that surface flaw fracture is influenced by the presence of an in-flaw-plane shear stress. If this were not the case, σ_n/σ_o would equal one, independent of the

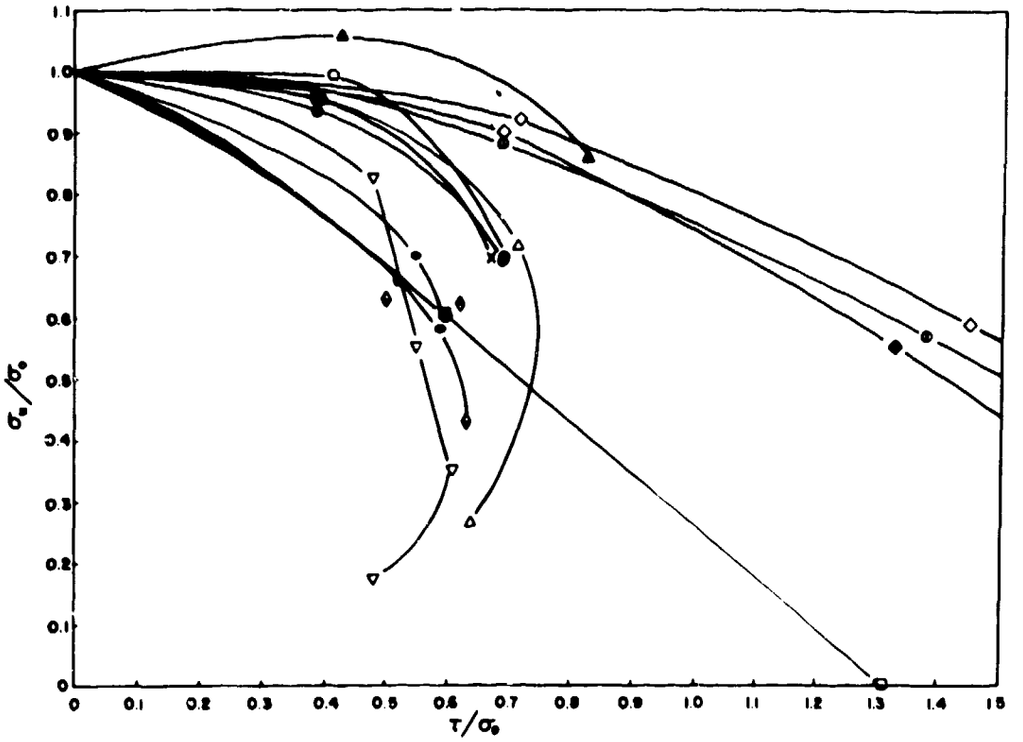

FIGURE 3: Mixed-Mode Fracture Results for Indentation Surface Flaws.

value of τ/σ_o. The data in Figure 3 clearly demonstrate that a constant normal stress criterion for fracture will be seriously in error, and that the fracture criterion must include mixed-mode loading conditions.

The data in Figure 3 for various ceramic materials and loading configurations exhibit a fairly wide range, rather than lying on a single curve. Most of the data comes from the fracture of inclined surface flaws in bending (13, 14, 15, 17, 18, 19, 20). Even within this single loading configuration, the data spread is significant. At very steep angles of inclination to the bending tensile stress, both σ_n and τ exhibit decreases at flaw fracture, which usually occurs only from the surface tip of the Knoop indentation.

The filled data points in Figure 3 indicate surface flaws which were annealed to remove indentation residual stresses prior to mixed-mode fracture. Marshall (17) has shown that the presence of these residual stresses leads to stable non-coplanar crack growth prior to catastrophic fracture under mixed-mode loading conditions. This change in crack shape might be expected to complicate the local mixed-mode fracture situation. However, the data in Figure 3 do not provide a clear-cut description of residual stress effects on mixed-mode fracture, with some data showing significant effects on σ_n and τ at fracture and other data showing little effect.

Mixed-mode fracture studies of surface flaws have been performed in combined tension/torsion (16,19) and diametral compression (18). For

TABLE 1. Key for Indentation Surface Flaw Mixed-Mode Fracture Results in Figure 3

Sym.	Material	Test Type	Indentation Conditions	Indentation Annealing	Ref.
	Hot-Pressed Si_3N_4*	Bending	59N Knoop	2h/1200°C	20
	Hot-Pressed Si_3N_4*	Bending	59N Knoop	None	19
	Hot-Pressed Si_3N_4*	Tension/ torsion	59N Knoop	1h/1300°C	19
	Hot-Pressed Si_3N_4*	Tension/ torsion	59N Knoop	None	16
	Hot-Pressed Si_3N_4**	Bending	25N Knoop	None	13, 14
	Soda-Lime Glass	Bending	20N Knoop	None	15
	Hot-Pressed Si_3N_4**	Bending	50N Knoop	4h/1200°C	17
	Hot-Pressed Si_3N_4**	Bending	50N Knoop	None	17
	Pyroceram 9606	Diametral Compression	50N Knoop	None	18
	Pyroceram 9606	Diametral Compression	50N Knoop	4h/820°C	18
	AVCO Al_2O_3	Diametral Compression	50N Knoop	None	18
	Pyroceram 9606	Bending	50N Knoop	None	18
	Pyroceram 9606	Bending	50N Knoop	4h/820°C	18
	AVCO Al_2O_3	Bending	50N Knoop	None	18

*Ceradyne 147A Si_3N_4
**Norton NC-132 Si_3N_4

these loading configurations, fracture under pure shear conditions (i.e., zero normal stress on the flaw plane) is possible. For as-indented flaws in hot-pressed Si_3N_4, the author obtained a value of $\tau/\sigma_o = 1.31$ for this condition of surface flaw fracture, although this value may have been influenced by non-coplanar stable crack extension prior to catastrophic failure in pure torsion. Shetty et al. (18) report τ/σ_o values in pure shear of 2.0-2.2 for Pyroceram 9606 and Al_2O_3. They have also indicated a significant difference in the dependence of σ_n/σ_o on τ/σ_o between diametral compression and bending which they ascribe to a stress-state effect.

Large Cracks

The only large crack mixed-mode fracture data presently available for a ceramic material are shown in Figure 4. In this investigation (20), the Mode I-II fracture of hot-pressed Si_3N_4 was examined using circumferentially slotted tubes in combined tension/torsion, while Mode

I-III fracture was studied using circumferentially notched rods in combined tension/torsion.

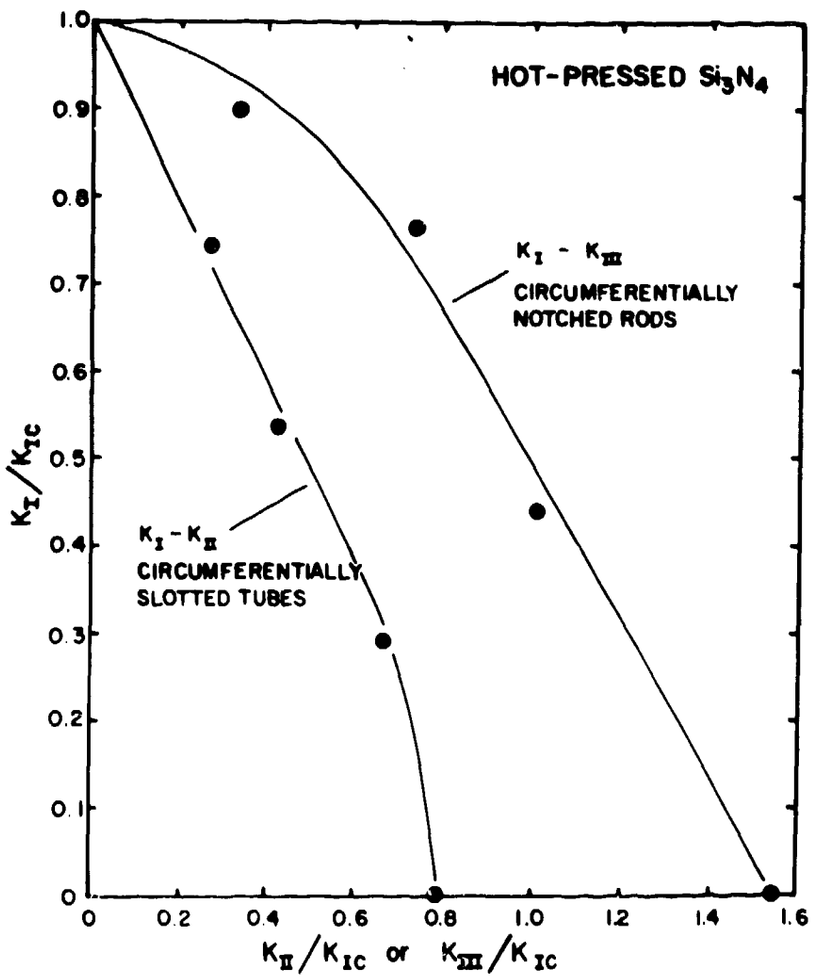

FIGURE 4: Mixed-Mode Fracture of Large Cracks in Hot-Pressed Si_3N_4.

As may be seen in Figure 4, both Mode II and Mode III influence Mode I fracture, with Mode II conditions having a greater influence. Ueda et al. (21) have observed similar trends for the mixed-mode fracture of brittle polymethylmethacrylate (PMMA). Observed stress intensity factor ratios in Si_3N_4 for pure Mode II and pure Mode III loading were $K_{IIC}/K_{IC} = 0.79$ and $K_{IIIC}/K_{IC} = 1.55$. For the mixed-mode fracture of these large cracks, non-planar fracture was universally observed, as has also been the case for surface flaws. The theoretical non-coplanar fracture theories almost universally predict K_{IIC}/K_{IC} and K_{IIIC}/K_{IC} ratios less than one (20).

With regard to large crack studies on other brittle materials, Awaji and Sato (22) have reported K_{IIC}/K_{IC} ratios in the range of 1.09-1.16 using inclined large cracks in diametral compression for graphite, plaster, and marble materials. For brittle PMMA (21), K_{IIC}/K_{IC} ratios in the range of 0.75-0.9 and K_{IIIC}/K_{IC} ratios of 0.98 have been observed. In metals, various studies (23-26) have indicated K_{IIC}/K_{IC} ratios in the range of 1.0-1.2, with K_{IIIC}/K_{IC} ratios in the neighborhood of 1.2 (23,26).

Comparison of Surface Flaws and Large Cracks

Figure 5 compares experimental values of K_I/K_{IC} versus K_{II}/K_{IC} for circumferentially slotted tubes and annealed Knoop surface flaws in hot-pressed Si_3N_4 (20). Also shown for comparison are a number of

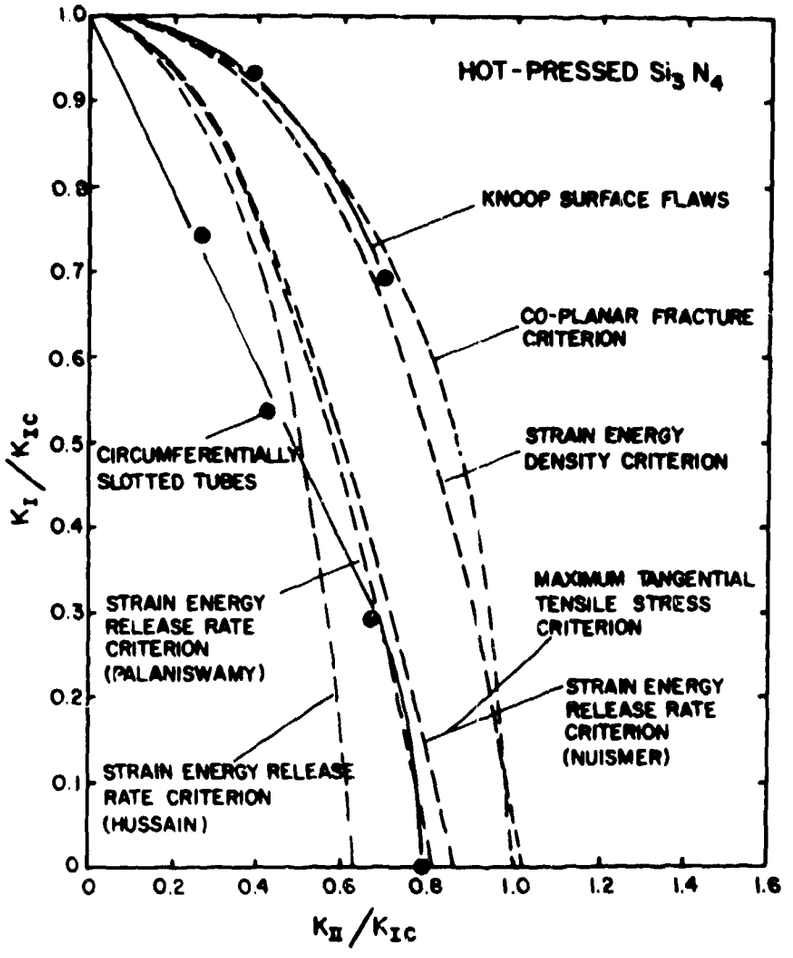

FIGURE 5: Comparison of the Mixed-Mode Fracture of Circumferentially Slotted Tubes and Annealed Surface Flaws in Hot-Pressed Si_3N_4.

mixed-mode fracture criteria. As may be seen, the mixed-mode fracture data for circumferentially slotted tubes and Knoop surface flaws do not coincide. In general, the surface flaw data exhibits less of an effect of K_{II} on K_I fracture than does the slotted tube data. While the slotted tube data are best described by predictions of the non-coplanar strain energy release rate (5,6,8) and maximum tangential tensile stress (11) criteria, the surface flaw results are best described by the coplanar fracture (4) and strain energy density (12) criteria. Previous investigations (14,17) have also indicated that the mixed-mode fracture of surface flaws is well described by the coplanar fracture criterion, this despite the fact that the fracture response is clearly non-coplanar.

DISCUSSION

The difference in the mixed-mode responses of large cracks and surface flaws shown in Figure 5 is of some insight. Marshall (17) has suggested that surface flaws which are free of indentation residual stresses (i.e., annealed flaws) have crack surfaces that are in contact at asperities. This resistance to shear at the contact points would reduce the effectiveness of the applied shear loading in producing stress intensification at the crack tip, thus effectively reducing the actual K_{II} level for surface flaws under mixed K_I/K_{II} loading below that calculated under the assumption that the surfaces were not in contact. Since the large crack surfaces were not in contact, this would account for the difference in Figure 5.

In a recent study (20), this effect has been modeled by assuming that the in-flaw-plane shear stress for surface flaws is reduced by a multiplicative factor related to the surface roughness and crack opening displacement of the flaw, termed the shear resistance factor S_R. This factor ranges between zero (complete crack resistance to sliding displacements) and one (no crack resistance effects). A likely functional form for the shear resistance factor is the ratio of the surface flaw crack opening displacement (COD) to the average asperity height d. Using the expression of Sneddon (27) for the elastic crack opening displacement of a penny-shaped flaw in an infinite medium under tensile loading, the Mode II stress intensity factor for surface flaws may be expressed as

$$K_{II} = \left(\frac{4}{\pi^{1/2}(2-\nu)}\right) \left(\frac{8(1-\nu^2)\ \sigma_n\ a}{\pi\ Ed}\right) \tau\ a^{1/2}$$

where the second term represents the shear resistance factor. Here, σ_n is the stress normal to the flaw plane, a is the flaw radius, τ is the applied shear stress, E is the elastic modulus, d is the asperity height, and ν is Poisson's ratio.

The above expression indicates that K_{II} for surface flaws depends on both the shear stress τ and the normal stress σ_n. In addition, the flaw size dependence of K_{II} becomes $a^{3/2}$ rather than $a^{1/2}$. Finally, the material variables of elastic modulus E and asperity height d (expected to be some fraction of the material grain size) are introduced. These would suggest that ceramics with high elastic moduli and large grain sizes may be the most susceptible to shear resistance effects. Application of the above expression to mixed-mode surface flaw fracture in hot-pressed Si_3N_4 (20) brings surface flaw responses into better correspondence with the predictions of non-coplanar strain energy release rate fracture theories.

SUMMARY

Experimental mixed-mode fracture responses for ceramics and other brittle materials have been reviewed and compared to predictions of theoretical mixed-mode fracture criteria. Surface flaw results demonstrate a significant effect of in-flaw-plane shear stresses on the flaw-plane normal stress at fracture, indicating that the surface flaw fracture criterion must include mixed-mode loading conditions. Mixed-mode fracture studies of large cracks suggest that Mode II has a greater effect on Mode I fracture than does Mode III. A comparison of surface

flaw and large crack mixed-mode I-II fracture behavior indicates that shear resistance effects influence the surface flaw mixed-mode response.

REFERENCES

1. S. B. Batdorf and J. G. Crose, J. Appl. Mech., 41:459 (1974).
2. S. B. Batdorf and H. L. Heinisch, J. Amer. Ceram. Soc., 61:355 (1978).
3. K. T. Faber and A. G. Evans, Acta Met., 31:565 (1983).
4. P. C. Paris and G. C. Sih, in "Stress Analysis of Cracks", ASTM STP 381, American Society for Testing and Materials (1965).
5. M. A. Hussain, S. L. Pu, and J. Underwood, in "Fracture Analysis", ASTM STP 560, American Society for Testing and Materials (1974).
6. R. J. Nuismer, Int. J. Fract., 11:245 (1975).
7. W. T. Chiang, in "Fracture 1977", 4:135, University of Waterloo (1977).
8. K. Palaniswamy and W. G. Knauss, in "Mechanics Today", 4:87, S. Nemat-Nasser, ed., Pergamon Press, New York (1978).
9. M. Ichikawa and S. Tanaka, Int. J. Fract., 18:19 (1982).
10. W. Shen and J. D. Lee, Eng. Fract. Mech., 16:783 (1982).
11. F. Erdogan and G. C. Sih, J. Basic Eng., Trans. ASME, Series D, 85:519 (1963).
12. G. C. Sih, Int. J. Fract., 10:305 (1974).
13. J. J. Petrovic and M. G. Mendiratta, J. Amer. Ceram. Soc., 59:163 (1976).
14. J. J. Petrovic and M. G. Mendiratta, J. Amer. Ceram. Soc., 60:463 (1977).
15. S. W. Freiman, A. C. Gonzalez, and J. J. Mecholsky, J. Amer. Ceram. Soc., 62:206 (1979).
16. J. J. Petrovic, in "Fracture Mechanics of Ceramics", 6:63, R. C. Bradt, A. G. Evans, D. P. H. Hasselman, and F. F. Lange, eds., Plenum Publishing Corp., New York (1983).
17. D. B. Marshall, J. Amer. Ceram. Soc., 67:110 (1984).
18. D. K. Shetty, A. R. Rosenfield, and W. H. Duckworth, "Biaxial Stress-State Effects on Mixed-Mode Fracture from Surface Flaws in Ceramics", submitted to the J. Amer. Ceram. Soc., (1985).
19. J. J. Petrovic, unpublished research.
20. J. J. Petrovic, "Mixed-Mode Fracture of Hot-Pressed Si_3N_4", J. Amer. Ceram. Soc., June (1985).
21. Y. Ueda, K. Ikeda, T. Yao, and M. Aoki, Eng. Fract. Mech., 18:1131 (1983).
22. H. Awaji and S. Sato, J. Eng. Mat. & Tech., 100:175 (1978).
23. R. C. Shah, in "Fracture Analysis", ASTM STP 560, American Society for Testing and Materials (1974).
24. A. F. C. Liu, AIAA Journal, 12:180 (1974).
25. D. L. Jones and D. B. Chisholm, Eng. Fract. Mech., 7:261 (1975).
26. L. P. Pook, Eng. Fract. Mech., 3:205 (1971).
27. I. N. Sneddon, Proc. Roy. Soc. London, Series A, 187:229 (1946).

ACKNOWLEDGEMENTS

This work was supported by the Division of Materials Sciences, Office of Basic Energy Sciences, U. S. Department of Energy, under Contract No. W-7405-ENG-36. The author is grateful to M. L. Lovato for assistance in the performance of mixed-mode fracture testing.